Solid State Phenomena
ISSN: 1662-9779, Vol. 376, pp 71-77
doi:10.4028/p-H8wzJA

Submitted: 2024-09-16
Revised: 2025-05-16
Accepted: 2025-05-16
Online: 2025-09-10

How to Simulate Bipolar Degradation by UV Irradiation with High Accuracy

Yasuyuki Igarashi[1,a*], Kazumi Takano[1,b],
Yohsuke Matsushita[1,c], Takuya Morita[1,d]

[1]ITES Co., Ltd., 1-60 Kuribayashi, Otsu, Shiga 520-2151, Japan

[a]yiga@ites.co.jp, [b]kazumi_takano@ites.co.jp,
[c]yohsuke_matsushita@ites.co.jp, [d]takuya_morita@ites.co.jp

Keywords: basal plane dislocation, single Shockley stacking fault, carrier lifetime, photoluminescence, UV irradiation, bipolar degradation, screening, recombination-enhanced dislocation glide.

Abstract. The reliability issue of the bipolar degradation in 4H-SiC devices has not been completely eliminated. We have been proposing a screening method for latent defects causing this reliability issue utilizing UV irradiation, which we call the E-V-C (Expansion-Visualization-Contraction) method. This method is based on the property that the REDG (recombination-enhanced dislocation glide) mechanism that causes the bipolar degradation can be reproduced by UV irradiation. However, in order to apply this method as a screening method, accurate quantification of the correlation between current density in forward bias and UV irradiance is required. In this article, we estimated the extent to which the carrier lifetime of the sample affects the quantification of the correlation and found that it had a non-negligible degree of influence on the correlation. Then, we tried to find if there is a simple method for estimating carrier lifetime that can be incorporated in the screening process, and report on our attempts in progress.

Introduction

4H-SiC devices, which are widely used in products today, have been found to have a reliability issue of so-called bipolar degradation for more than 20 years. The degradation is caused by the nucleation and expansion of a 1SSF (single Shockley stacking fault), originating from BPD (basal plane dislocation) which exists in the epilayer or near the epilayer and the substrate (epi/sub) interface. The 1SSFs are expanded by the electron–hole recombination energy when excessive minority carriers are injected into the regions in the vicinity of the BPDs, which is called REDG mechanism. Various process improvements have been made to convert BPD to benign dislocation TED (threading edge dislocation) at the epilayer/substrate interface, which does not expand. However, it is known that at high current densities, expansion occurs from the BPD-to-TED conversion point, and the issue has not yet been fully resolved.

Since a TED-converted BPD is difficult to identify with existing mass-production inspection system, we have proposed the E-V-C method as a means of screening the latent defects, TED-converted BPDs [1]. The E-V-C method is a technique to visualize and screen TED-converted BPDs by utilizing UV irradiation and PL observation, aiming for replacing the time-consuming “burn-in” screening usually conducted by overcurrent stress. In order to make the use of UV irradiation to be useful and practical as a screening method, it is required that the UV irradiation conditions must match the specifications of each product, specifically, the absolute maximum current rating of the product. This is because, if UV irradiance is unnecessarily intense, even devices that would not show any degradation within the rated current in normal usage will be screened out (overkill). Therefore, it is essential to derive an accurate quantitative correlation between the forward bias conditions and UV irradiation conditions. It has been reported that whether or not TED-converted BPD expands into a bar shaped stacking fault depends on whether the hole density near the conversion point exceeds a certain threshold during forward biasing [2]. In other words, the key parameter for deriving UV

irradiation conditions equivalent to forward bias conditions is the hole density in the vicinity of the conversion points. On this basis, the authors' team has been exploring the derivation of quantitative correlations [3].

The variable that determines the hole density is the current density in the case of forward biasing and the irradiance in the case of UV irradiation, so relating the two is the point. In addition to these variables, however, there are other parameters that affect the hole density and differ from sample to sample. They include the carrier lifetime of the drift layer in both forward bias and UV irradiation, and surface and interface recombination velocities of the drift layer in UV irradiation. In this article, we first estimated how much difference in correlation appeared when the carrier lifetime was varied. As a result, it was found that a certain amount of non-negligible difference in correlation appeared when the carrier lifetime was incorrectly estimated. This means that it is required to find a simpler method to estimate the carrier lifetime than the μ-PCD or TRPL method, which is commonly used, since it is not realistic to apply either of those methods to all wafers in production line. We referred to the literature that has evaluated the relationship between PL (photoluminescence) intensity and carrier lifetime [4]. In the latter part of this article, we report on our attempt to estimate carrier lifetime by PL intensity measurement. If the carrier lifetime can be estimated by PL intensity measurement, it can be applied to the production process.

Estimation of the Influence of Carrier Lifetime on the Correlation between Current Density and UV Irradiance

First, UV irradiation condition that is equivalent to forward biasing is derived. In the case of a PiN diode, the current flow inside the drift layer consists of hole injection from the anode p+ diffusion layer and electron injection from the n+ buffer layer (or n+ substrate if there is no buffer layer), and the density of the excess minority carrier (hole) in the drift layer can be expressed as follows [5, 6].

$$\Delta p_{FB}(x) = \frac{J\eta_i\tau_i}{2qL_a}\left[\frac{\cosh\left\{\left(x-\frac{W}{2}\right)/L_a\right\}}{\sinh\left\{\left(\frac{W}{2}\right)/L_a\right\}} - B'\frac{\sinh\left\{\left(x-\frac{W}{2}\right)/L_a\right\}}{\cosh\left\{\left(\frac{W}{2}\right)/L_a\right\}}\right]. \quad (1)$$

$where\ x: distance\ from\ p+/drift\ interface,\quad J: current\ density$
$\eta_i: recombination\ current\ density\ ratio\ in\ drift\ layer$
$\tau_i: carrier\ lifetime\ in\ drift\ layer,\quad W: drift\ layer\ thickness$
$L_a: ambipolar\ diffusion\ length,\quad q: elementary\ charge$
$B': shape\ factor$

Here, the shape factor *B'* is calculated by

$$B' = \frac{1}{\eta_i}\left(B + \eta_{nh} - \eta_{pe}\right), \quad B = \frac{\mu_{ie}/\mu_{ih} - 1}{\mu_{ie}/\mu_{ih} + 1}. \quad (2)$$

$where\ \eta_{nh}: hole\ current\ density\ ratio\ at\ drift/buffer\ interface$
$\eta_{pe}: electron\ current\ density\ ratio\ at\ p+/drift\ interface$
$\mu_{ih}: hole\ mobility\ in\ drift\ layer,\quad \mu_{ie}: electron\ mobility\ in\ drift\ layer$

$$here \quad \eta_i + \eta_{nh} + \eta_{pe} = 1. \quad (3)$$

The electron current density $J \cdot \eta_{pe}$ at the p+/drift interface and the hole current density $J \cdot \eta_{nh}$ at the drift/buffer interface can be expressed by the following equations using Eq. 1.

$$J\eta_{pe} = q\frac{D_{pe}}{L_{pe}}\coth\left(\frac{W_p}{L_{pe}}\right)\frac{\{\Delta p_{FB}(0)\}^2}{N_a}. \quad (4)$$

$$J\eta_{nh} = q\frac{D_{nh}}{L_{nh}}\coth\left(\frac{W_n}{L_{nh}}\right)\frac{\{\Delta p_{FB}(W)\}^2}{N_d}. \quad (5)$$

where D_{pe}: *electron diffusion coefficient in* $p+$ *layer*
D_{nh}: *hole diffusion coefficient in buffer layer*
L_{pe}: *electron diffusion length in* $p+$ *layer*
L_{nh}: *hole diffusion length in buffer layer*
W_p: $p+$ *layer thickness,* W_n: *buffer layer thickness*
N_a: $p+$ *layer acceptor density,* N_d: *buffer layer donor density*

Eventually, Eq. 2 to Eq. 5 become simultaneous equations in four unknowns concerning B', η_i, η_{nh}, and η_{pe}, and B' can be obtained by a numerical solution method.

On the other hand, the calculation of the hole density generated by UV irradiation using a pulsed laser has been reported by the authors' team [3]. The hole density generated by a single UV pulse irradiation is given as a function of depth *x* and time *t* in the drift layer in the form of the Fourier series [7, 8] as follows.

$$\Delta p_{UV}(x,t) = \sum_{n=1}^{\infty}\Gamma_n\Phi_n(x)F_n(t). \quad (6)$$

where $\Phi_n(x)$ *are spatial functions with parameters of drift layer width, surface/interface recombination velocities and ambipolar diffusion coefficient.*
$F_n(t)$ *are time dependent terms with parameters of ambipolar diffusion coefficient and lifetime in drift layer.*
Γ_n *are constants including initial hole density* g_0 *at* $x=0, t=0$ *and absorption coefficient* α *of excitation source (laser light).*

It is important to note that at time zero, immediately after irradiation, the hole density is described by

$$\Delta p_{UV}(x,0) = \sum_{n=1}^{\infty}\Gamma_n\Phi_n(x) = g_0\exp(-\alpha x). \quad (7)$$

where α *is an absorption coefficient of excitation source (laser light) and*
$g_0 = N_0\alpha(1-R)/(1-Re^{-\alpha W})$
here, N_0: *number of photons per unit area emitted from laser*
R : *reflectivity*
W: *drift layer thickness*

This means that *the hole density depth profile at time zero does not depend on the carrier lifetime and the surface / interface recombination velocities*. In other words, the hole density distribution at time zero immediately after irradiation is determined only by the injection amount g_0 and the absorption coefficient α. The carrier lifetime and surface / interface recombination velocities only affect the rate of decay of hole density (decay curve). From the above, since the key parameter for deriving equivalent forward bias conditions with UV irradiation is the hole density in the vicinity of the conversion points, the UV irradiation condition is so determined that the hole density at the drift/buffer interface becomes the same between UV irradiation and forward bias.

$$\Delta p_{FB}(W) = \Delta p_{UV}(W,0). \quad (8)$$

Next, considering the lifetime dependence on the hole density, since the right side in Eq. 8 is independent of the lifetime, the variation range of the correlation can be estimated by examining the left side lifetime dependence.

We calculated the effect of carrier lifetime on the hole density on a 6" 4H-SiC wafer with PiN diodes. The profile of the wafer was: anode p+ density 4×10^{18} cm^{-3} (0.5 μm thick), drift layer density 4×10^{15} cm^{-3} (9.1 μm thick), and n+ buffer layer density 1×10^{18} cm^{-3} (1.0 μm thick). The injection current density was assumed 300 A/cm^2, and depth profiles were calculated for carrier lifetime of τ = 380 ns, 130 ns (=1/3 × 380 ns), and 76 ns (=1/5 × 380 ns). Fig. 1 shows the results calculated by using Eq. 1 (solid lines), together with the calculated values by using the 1D device simulator, AFORS-HET (dashed lines).

The results show that the hole density at the drift/buffer interface decreases by more than 22% when the lifetime is reduced by 1/3 (380ns to 130ns) and by more than 37% when the lifetime is reduced by 1/5 (380ns to 76ns), indicating that knowing the lifetime of the drift layer is very important to improve the accuracy of the correlation Eq. 8.

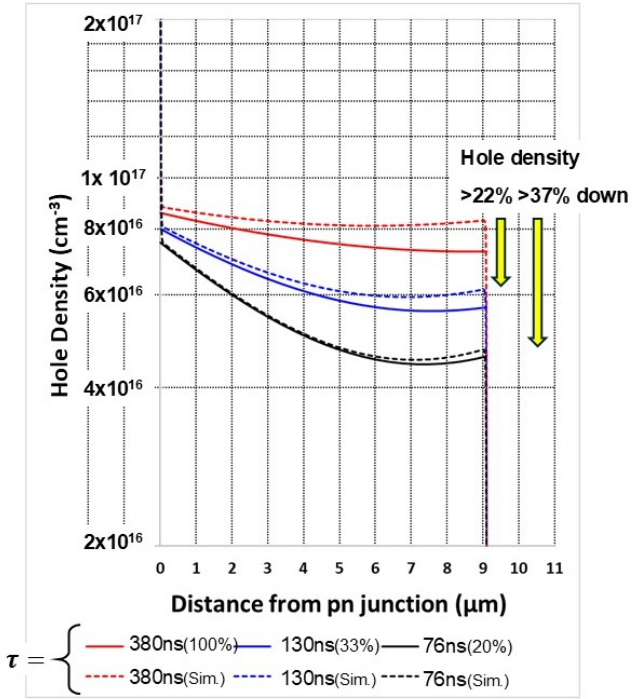

Fig. 1. Depth profiles of hole density in drift layer.

Trial on the Estimation of Carrier Lifetime by PL Intensity Measurement

In the screening process in production, it is not practical to use the μ-PCD method or TRPL method to inspect all the wafers because of a significant cost impact. Since there was a report that investigated the correlation between PL intensity and lifetime of wafers [4], we examined whether the lifetime could be estimated by measuring PL intensity.

Experiment - I (Preliminary): Defect Expansion Rate of 1SSF vs. PL Intensity

According to the literature [4], the PL intensity of 6H-SiC at 423 nm (related to band-to-band transitions) decreases almost in direct proportion to the shortening of the lifetime. Since the short lifetime means that there are many recombination centers in the drift layer, and the glide velocity of Si(g) core (1SSF expansion rate) is also expected to become low, the relationship between the glide velocity and PL intensity at 380 nm (related to 4H-SiC band-to-band transitions) was investigated.

The profiles of the three wafers with PiN diodes used in the measurements are shown in Table 1. (Wafer-B is the wafer referred in the previous section to estimate the carrier lifetime dependence on

the hole density.) The glide velocity of the Si(g) core in the ⟨1 $\bar{1}$ 0 0⟩ direction was measured as the expansion velocity in the forward biased PiN diodes, and PL spectra were obtained from three points in the vicinity of the diodes. The excitation source was a 355nm Nd:YAG laser, beam diameter 1mmΦ, 0.8W, 2sec. The measurement results of the glide velocity and the PL spectra are shown in Fig.2 and Fig.3, respectively. The PL intensity was in the order of Wafer C > A > B, and the difference between Wafer B and C is consistent with the difference in expansion speed although it is not significant between the two. While Wafer A is inconsistent with the glide velocity data because the emission would be further stronger if the epi thickness of Wafer A were as thick as that of the other two. This may be due to the fact that the number of defects sampled from Wafer A was very small. Anyway, no clear correlation between defect expansion rate and PL intensity at 380 nm was obtained from this experiment.

Table 1. Sample preparation.

Wafer ID	Size	p+ anode	n- drift layer	n+ buffer layer
A	4”	3×10^{18} cm^{-3}	5.4 μm, 5×10^{15} cm^{-3}	0.5μm, 1×10^{18} cm^{-3}
B	6”	3×10^{18} cm^{-3}	9.1μm, 4×10^{15} cm^{-3}	1.0μm, 1×10^{18} cm^{-3}
C	6”	3×10^{18} cm^{-3}	10.6μm, 7.7×10^{15} cm^{-3}	1.0μm, 1×10^{18} cm^{-3}

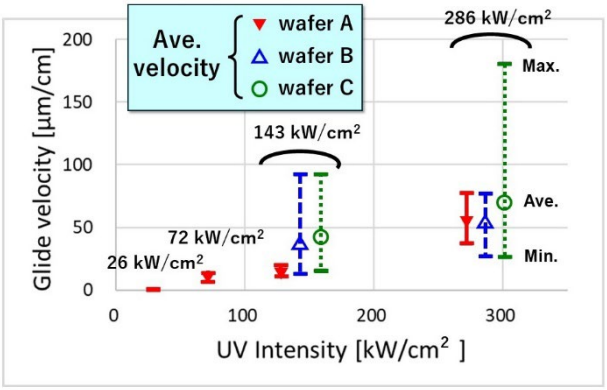

Fig. 2. Si(g) core glide velocity range per wafer.

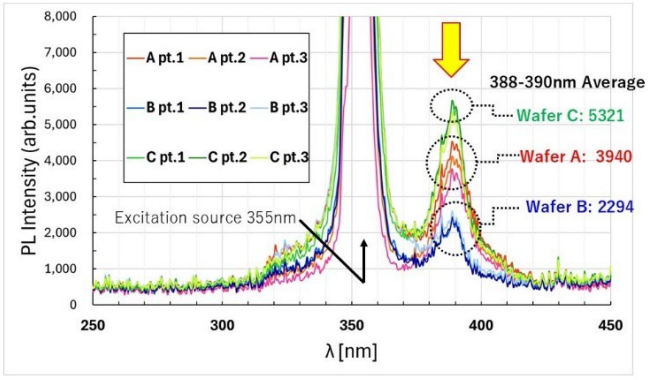

Fig. 3. PL luminescence peak for different wafers.

Experiment – II: Carrier Lifetime vs. PL intensity

PL spectrum was obtained on two 4H-SiC wafers. Each wafer was evenly divided into four regions and energy filtered implanted with N+ (Nitrogen) ions with different doses per region, and the carrier lifetime of each region was also measured by μ-PCD method. The measurement point of the PL spectrum and that of the lifetime are identical in each region. The excitation wavelength was 349 nm/26 GHz, and one of the four regions was without implantation. The PL spectrum was measured by a 355nm YAG laser with beam diameter 1mmΦ, 0.6W, 10sec. The measurement results are summarized in Table 2. An example of the obtained PL spectrum (Wafer ID:D) is shown in

Fig. 4, showing a peak at around 380-390 nm, along with another peak at around 490 nm, which may be due to drift layer doping with ion implantation process because of absence of this peak in the PL spectrum from the non-doped region.

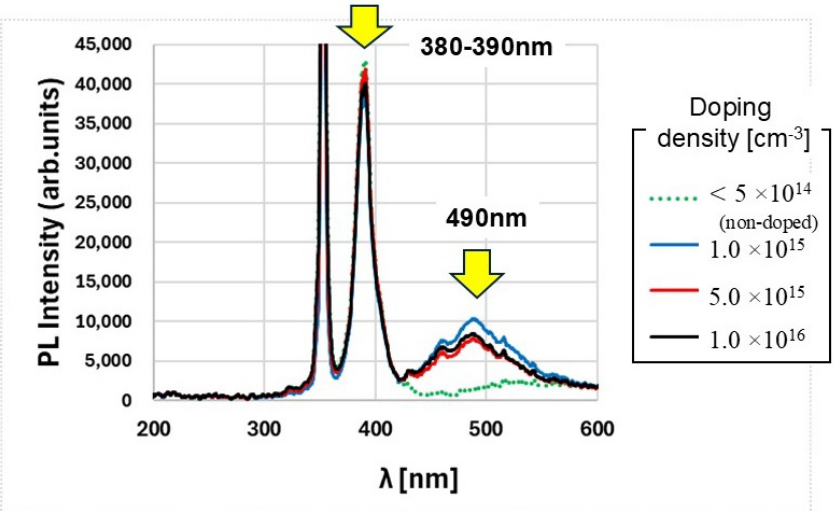

Fig. 4. PL spectrum for N+ ion implanted wafer (Wafer: D).

In μ-PCD measurement, the carrier lifetime decay curve can be divided into 1/e time region (fast decay) and $1/e^2$ time region (slow decay). Since the surface condition of the sample greatly affects the 1/e time, the $1/e^2$ lifetime was adopted as carrier lifetime here in this article. Fig. 5 shows a plot of PL intensity at 380-390 nm versus carrier lifetime. As shown in the figure, although there was clear difference in PL intensity between wafers, PL intensity was almost constant within the same wafer regardless of the $1/e^2$ carrier lifetime variation, indicating that there is no correlation between PL intensity at 380-390 nm and carrier lifetime. On the other hand, Fig. 6 plots the correlation between the lifetime and the PL intensity at around 490 nm, which is considered to be reflected by ion implantation. This shows a clear positive correlation between the lifetime and the PL intensity. The reason for the appearance of the peak at around 490 nm has not yet been scrutinized, and we would like to clarify its cause through further investigation.

In summary, contrary to initial expectations, it was difficult to estimate the carrier lifetime from the PL intensity at 380-390nm (reflecting band-to-band transitions of 4H-SiC), but a positive correlation between the PL intensity at around 490nm and the carrier lifetime was observed.

Table 2. Doping profile, lifetime and PL intensity.

Wafer ID	Doping Density [cm^{-3}]	1/e Time [ns]	$1/e^2$ Time [ns]	PL Intensity @ ~390nm (arb.units)	PL Intensity @ ~490nm (arb.units)
D	$<5 \times 10^{14}$ (non-doped)	160	107.5	42500	1500
	1.0×10^{15}	112.5	337.5	38500	10300
	5.0×10^{15}	72.5	220	41500	7800
	1.0×10^{16}	60	172.5	40000	8500
E	$<5 \times 10^{14}$ (non-doped)	177.5	135	26300	2000
	1.0×10^{15}	177.5	395	22000	11800
	5.0×10^{15}	92.5	207.5	23500	9500
	1.0×10^{16}	60	200	26000	8800

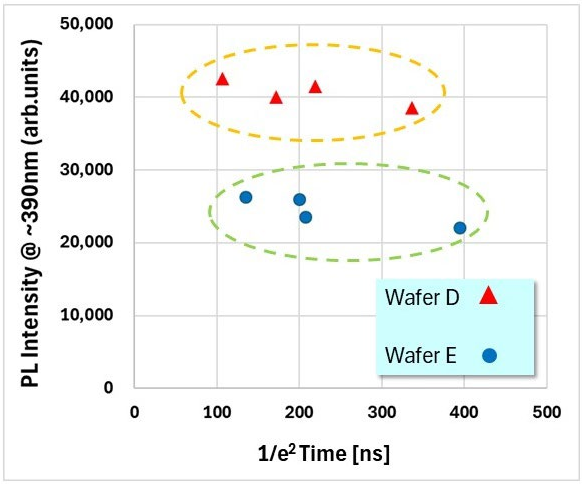

Fig. 5. Lifetime VS. PL intensity at ~390nm.

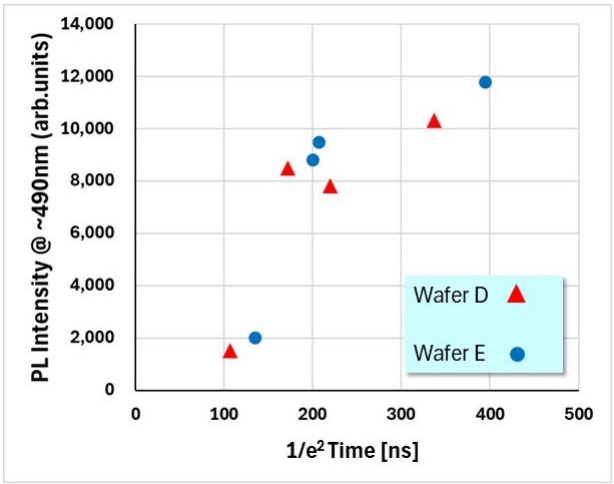

Fig. 6. Lifetime VS. PL intensity at ~490nm.

Summary

We evaluated the influence of carrier lifetime on quantification of correlation between current density during forward biasing and UV irradiance. As a result, it was found that reflecting the sample-specific carrier lifetime in the correlation equation would surely improve the accuracy of the correlation. To do this for every sample in production line, a simpler method for estimating carrier lifetime is required. We are investigating the possibility of estimating the carrier lifetime by measuring the PL intensity, but no useful data were obtained so far from the PL intensity at 380-390 nm (band-to-band transitions of 4H-SiC). On the other hand, we found a clear positive correlation between carrier lifetime and PL intensity at around 490 nm, which seemed affected by ion implantation process. Further analysis is required to clarify the reason for the 490nm peak of PL spectrum.

Acknowledgments

The authors wish to thank Hitesh Jayaprakash, mi2-factory GmbH, for providing us the 4H-SiC wafers for our PL observation and also providing us the carrier lifetime data of those samples.

References

[1] Y. Igarashi, K. Takano, Y. Matsushita, C. Shibata, Defect and Diffusion Forum 425, 75 (2023).

[2] T. Tawara, S. Matsunaga, T. Fujimoto, M. Ryo, M. Miyazato, T. Miyazawa, K. Takenaka, M. Miyajima, A. Otsuki, Y. Yonezawa, T. Kato, H. Okumura, T. Kimoto, and H. Tsuchida, J. Appl. Phys. 123, 025707 (2018).

[3] Y. Igarashi, K. Takano, Y. Matsushita, C. Shibata, Defect and Diffusion Forum 434, 23 (2024).

[4] R. Reitano, M. Zimbone, P. Musumeci, P. Baeri. Mater. Sci. Forum 483-485, p.373 (2005).

[5] A. Herlet, Solid-State Electron. 11, p.717 (1968).

[6] Y. Yamashita, Doctorial Paper, University of Tsukuba, April 2018, titled "Study on Structural Optimization of Pin Diodes for Power Applications" (in Japanese).

[7] Y. Ogita, J. Appl. Phys., 79, p.6954 (1996).

[8] S. Sumie, F. Ojima, K. Yamashita, K. Iba, and H. Hashizume, J. Electrochem. Soc. 152 G99 (2005).